

## Shear Melting of Colloids: A Nonequilibrium Phase Diagram

Mark J. Stevens and Mark O. Robbins

*Department of Physics and Astronomy, The Johns Hopkins University, Baltimore, Maryland 21218*

James F. Belak

*Lawrence Livermore National Laboratory, University of California, Livermore, California 94550*

(Received 7 February 1991)

Experiments show that charge-stabilized colloidal suspensions form crystals which can melt by applied shear stress. We present a molecular-dynamics simulation study of shear melting in colloids. The non-equilibrium phase diagram is calculated for a volume fraction which has an equilibrium fcc structure. The mechanism for flow in the sheared solid is found to be planes sliding over planes. We find that weak equilibrium solids (high added salt) shear melt, but strong equilibrium solids do not. Instead, shear produces a crossover to a new solid structure. This appears in the phase diagram as a reentrant solid phase. Results for shear stress and phase diagram are consistent with existing experiments.

PACS numbers: 62.20.-x, 64.70.Dv, 82.70.Dd

An understanding of the plastic deformation of solids is fundamental to materials science. Deformation at low shear rates is qualitatively understood in terms of the creep of dilute dislocations.<sup>1</sup> The mechanisms of deformation at high shear rates are different and not well understood. An understanding of these mechanisms is important for a wide variety of problems, including flow of the Earth's crust,<sup>1</sup> friction,<sup>2</sup> and shearing of colloids.<sup>3</sup>

High-shear-rate experiments on normal solids have been thwarted by the immense shear stress required. Recently, this difficulty has been overcome by studying the "soft" solids formed by charged monodisperse polystyrene spheres (polyballs) in solution.<sup>4</sup> Polyballs form equilibrium fcc, bcc, or fluid phases,<sup>4,5</sup> depending on the volume fraction of polyballs  $\phi$  and the concentration of added salt  $\rho_s$ . Increasing  $\phi$  strengthens interactions and favors solid phases. Increasing  $\rho_s$  screens interactions and favors the fluid phase. These polyball phases behave much like *atomic* matter. However, polyball radii and interparticle spacings are of the order of a micron. Since elastic moduli scale with density, polyball crystals are  $10^{12}$  times weaker than ordinary solids.<sup>4</sup>

Experimental work on sheared colloidal systems has focused on measurements of the structure factor<sup>3,6</sup>  $S(\mathbf{k})$  and of shear rate versus stress ( $\dot{\gamma}$ - $\sigma$ ) curves.<sup>7,8</sup> The sheared solid is found to undergo structural transformations with increasing shear rate.<sup>3,6</sup> In some cases, a novel first-order melting transition occurs.<sup>3,6-8</sup> The origin of this shear-melting transition is not yet understood.

In this Letter we present the first molecular-dynamics (MD) simulation study of shear melting in colloids. The  $(\rho_s, \dot{\gamma})$  phase diagram is calculated for a volume fraction where the equilibrium structure is fcc. The structure of the shearing solid is examined through calculation of the structure factor  $S(\mathbf{k})$  and through imaging of particle positions. Finally,  $\dot{\gamma}$ - $\sigma$  curves are calculated. Results are consistent with existing experimental data.

We chose system parameters corresponding to experiments by Lindsay and Chaikin,<sup>7,8</sup> who used 910-Å-diameter polyballs at  $\phi=0.04$ . The equilibrium  $(\phi, \rho_s)$  phase diagram and shear moduli of this system were well fitted by MD calculations<sup>5</sup> with a screened-Coulomb (Yukawa) potential for an effective polyball charge<sup>9</sup>  $Z^* \approx 450e$ .

Our simulations use the Slod<sup>10</sup> algorithm. A constant shear rate is applied by deforming the simulation cell uniformly in time in the shear direction  $\hat{v}$ . We denote the velocity gradient direction by  $\hat{V}$  and the remaining perpendicular direction by  $\hat{e}$ . For reasons outlined below, the simulation cell was allowed to shear along  $\hat{e}$  in response to internal stress using an extension of the Parrinello-Rahman (PR) method.<sup>11</sup> The number of particles  $N$  ranged from 768 to 2304.

Previous work on sheared systems has shown that simulation results may depend on the method used to maintain constant temperature. To test for such effects we used both the Nosé-Hoover and Berendsen algorithms.<sup>12,13</sup> In sheared systems, the thermal kinetic energy is defined relative to the mean flow. In some simulations we assumed that this was Couette flow, but it need not be<sup>14</sup> at high  $\dot{\gamma}$ . Thus, we have also implemented the profile unbiased thermostat (PUT) which calculates the mean flow self-consistently. Except as noted, all algorithms gave the same results within our accuracy.

The dimensionless quantity measuring the effect of shear is the Deborah number,  $De$ , which equals the shear rate times a relaxation time.<sup>15</sup> Since our MD simulations involve ballistic motion, the relevant relaxation time is the Einstein period,  $2\pi/\omega_E$ . The experimental systems are overdamped because of the surrounding water. The relevant relaxation time is  $\tau_{\text{diff}} = a_0^2/6D$ , the time for a free particle to diffuse a typical interparticle spacing  $a_0 = n^{-1/3}$ , where  $n$  is the particle density and  $D$  is the diffusion constant.<sup>8</sup> Our studies extended to  $De$

$\sim 0.7$  which is slightly larger than the range studied in experiments. While ballistic and diffusional dynamics may in principle lead to different behavior, our studies indicate that only  $De$  is relevant. Note that hydrodynamic forces in the experimental systems are negligible. Their ratio to the Yukawa interactions is of order

$$f = 6De(\phi^{-1/6} - \phi^{1/6})^{-2}kT/m\omega_E^2 a_0^2.$$

For our parameters,  $f < 0.02$  when  $De < 1$ .

One important experimental observation is that shear melting has a strong orientational dependence.<sup>6</sup> Shear aligns the close-packed planes perpendicular to  $\hat{V}$ , with the close-packed direction in the planes parallel to  $\hat{v}$ . Crystallites with different orientations melt and recrystallize with the preferred alignment. The special feature of this orientation is that planes of particles slide most readily over each other. The interplanar distance is maximized, and particles glide between lines of particles in neighboring planes. Our simulations reproduce this strong orientational character. Solids sheared in a different direction melt at extremely low shear rates. Results presented below are for the preferred orientation.

One method for determining the melting point is from the values of  $De$  where a solid phase melts or a liquid phase freezes. Since melting is a first-order phase transition, there may be a large difference between these values in small simulation cells. To obtain a more accurate melting line, simulations were performed on a system initially composed of a solid half and a fluid half. The stable phase at a given  $(\rho_s, De)$  is the one that grows to fill the simulation cell. This method gives an equilibrium melting transition at  $\rho_s = 31 \pm 1 \mu\text{M}$  which agrees with results of recent free-energy calculations.<sup>16</sup> The phenomenological Lindemann<sup>5</sup> criterion gives a slightly larger value:  $\rho_s = 37 \mu\text{M}$  for  $Z^* = 450e$ . Both values are smaller than the experimental value  $\rho_s \sim 50 \mu\text{M}$ . Quantitative agreement could be improved by increasing the

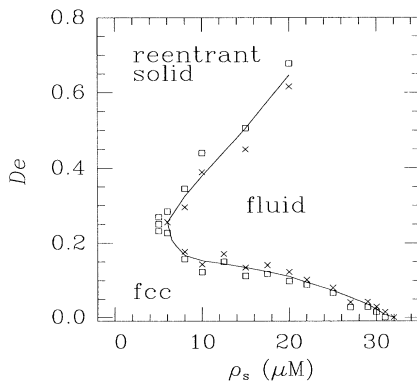


FIG. 1. Nonequilibrium phase diagram of sheared colloidal solids. Bounds on the transition line (solid) are indicated by the symbols. Squares (crosses) indicate systems that crystallized (melted).

unknown parameter  $Z^*$ , but we focus here on qualitative results which are not sensitive to such details.

The calculated nonequilibrium phase diagram shown in Fig. 1 has several surprising features. One is that the value of  $\rho_s$  at melting decreases roughly linearly as  $De$  increases from zero. This is consistent with recent experiments,<sup>17</sup> but density-functional calculations had predicted a  $De^{1/2}$  dependence.<sup>18,19</sup> Most surprising are the reentrant transition to a solid structure at high shear rates and the absence of melting at small  $\rho_s$ . We have checked that these features of the phase diagram are independent of our thermostat, although the shear rate at the reentrant freezing transition may vary by 10%. For all thermostats, fluid configurations crystallize rapidly in the reentrant regime. Experiments<sup>8</sup> also showed no melting transition below some  $\rho_s$ . No reentrant solid phase was observed, since the shear rate was not increased far enough above the melting transition.

These experiments determined the stable phase from shear-rate-stress curves. The measured  $\dot{\gamma}$ - $\sigma$  curves<sup>8</sup> are very similar to our calculated curves shown in Fig. 2. At equilibrium coexistence ( $\rho_s = 31 \mu\text{M}$ ) a pronounced non-Newtonian response is found in the fluid phase—the viscosity decreases with increasing  $De$ . As shown, the results for smaller  $\rho_s$  (solid phase) collapse onto a single curve at low and high  $De$  if the stress is normalized by the equilibrium shear modulus  $c_{44}$ . There is an apparent yield stress of  $\sigma_y = 0.016c_{44}$  as  $De \rightarrow 0$ . Experimental results<sup>20</sup> were normalized by the measured polycrystalline shear modulus  $G$ , and indicated  $\sigma_y = 0.035G$ . Since the calculated<sup>5</sup> ratio  $G/c_{44} \cong 0.5$  for these systems, the values are consistent. We found a similar value of  $\sigma_y/c_{44}$  for Lennard-Jones interactions.<sup>2</sup>

The melting transition appears in Fig. 2 as a discontinuous increase in  $\sigma$  with increasing  $De$ —the solid phase has a lower viscosity than the fluid. In the preferred crystal orientation, particles are aligned to slide smoothly past each other, while the disordered fluid structure leads to frequent “collisions.” As in experi-

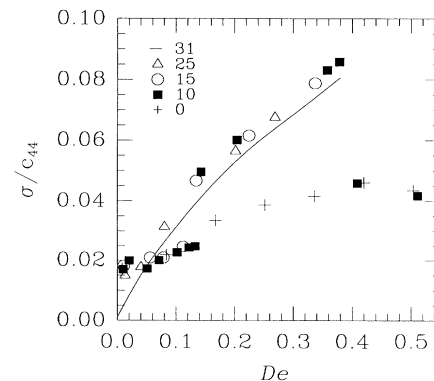


FIG. 2. The normalized shear-rate-stress curves for selected  $\rho_s$ . Statistical errors are of order 10%.

ments,  $\sigma$  increases by roughly a factor of 2 at melting. The response of the melted phase falls on a nearly universal fluid curve. No melting is seen in the data for  $\rho_s = 0$ . Reentrant freezing for  $\rho_s = 10 \mu\text{M}$  is indicated in Fig. 2 by a drop in the stress at  $De \sim 0.45$ .

Experimental values<sup>7,8</sup> of  $\dot{\gamma}$  at melting ranged up to about 150 Hz. Since  $\tau_{\text{diff}} = 1.5$  msec, this corresponds to  $De \cong 0.23$  which is roughly equal to our highest melting transitions ( $\sim 0.25$ ). This level of agreement may be fortuitous since the appropriate relaxation time for  $De$  is only defined up to a constant of order unity. However, the simulations clearly reproduce the orders of magnitude of the relevant stresses and shear rates.

Having shown that our simulations model the experiments reasonably well, we turn our attention to the shear-flow mechanism. Possible flow mechanisms in the solid phase include planes sliding over planes, vacancy motion, dislocation motion, and grain-boundary sliding. The orientational dependence<sup>6</sup> of shear melting suggests that plane-over-plane sliding dominates at these high shear rates. We have verified that the preferred orientation gives the minimum stress for plane-over-plane sliding. The fcc close-packed planes stack in an  $ABC$  sequence along  $\hat{v}$ . Figure 3 shows the path of minimal stress followed by particles in a plane sliding over an  $A$  plane. As discussed by Ackerson *et al.*,<sup>6</sup> the path is a zigzag line between positions corresponding to  $B$  and  $C$  planes. If all planes slide at the same rate, the structure alternates from one fcc stacking sequence ( $ABC \dots$ ) to its twin ( $ACB \dots$ ). We allowed our simulation cell<sup>11</sup> to shear along  $\hat{e}$ , so the solid could follow this path. The maximum stress along this minimal path,  $\sigma_{\text{max}} = 0.04c_{44}$  occurs where the straight line (dotted) meets the zigzag path in Fig. 3. The observed solid shear stresses are comparable ( $0.016c_{44}$  to  $0.045c_{44}$ ), and thus consistent with plane-over-plane sliding as the mechanism for shear.

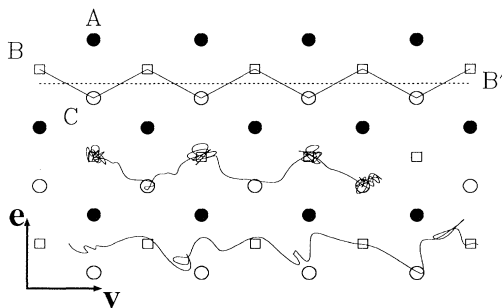


FIG. 3. Trajectory of the interplane displacement  $\Delta\mathbf{x}$  over an  $A$  plane. The solid line at the top shows the minimal path between  $B$  and  $C$  positions for a  $T=0$  crystal. Below is a trajectory for  $\rho_s = 10 \mu\text{M}$  at  $De = 0.02$ . The bottom trajectory is for  $De = 0.13$  (just below melting). The dotted line is the straight-line trajectory found for  $\sigma \gg \sigma_{\text{max}}$ . We call this plane position  $B'$ .

Examination of particle motions in our simulations bears out this conclusion, but shows that planes move incoherently. At low  $De$ , particles lie in close-packed planes normal to  $\hat{v}$ . Figure 3 shows a typical trajectory of the differential displacement between two planes,  $\Delta\mathbf{x}$ , at  $De = 0.02$ . The zigzag motion along the minimal path is clearly evident. In addition, prolonged sticking at the fcc positions corresponding to  $B$  or  $C$  stacking is exhibited. Plots of  $\Delta\mathbf{x}$  versus time show jerky motion—a succession of rapid jumps separated by plateaus of different length. Jumps of different planes occur incoherently, disrupting the stacking sequence. This is not surprising given that the applied stress is less than  $\sigma_{\text{max}}$ . Thermal fluctuations are required to allow interplane sliding.

As the shear rate increases, the trajectory deviates from the minimal path and there is less time for planes to lock (Fig. 3). For  $\rho_s > 5 \mu\text{M}$  the planes become increasingly disordered and eventually melt. The onset of melting coincides with loss of layering normal to  $\hat{v}$ . For  $\rho_s < 5 \mu\text{M}$ ,  $\sigma$  reaches  $\sigma_{\text{max}}$  at  $De \sim 0.25$ . Above this  $De$  all planes can slide freely. Shear becomes an ordering force—displacements about the close-packed positions decrease to eliminate collisions between neighboring planes. At higher  $\rho_s$ , the reentrant solid phase results.

The value of  $\sigma$  actually *decreases* with increasing  $De$  for  $De > 0.4$ . This leads to one of the few observed thermostat-dependent results. Using the “biased” thermostat which assumes Couette flow, we find  $\Delta\mathbf{x}$  approaches the straight-line trajectory shown in Fig. 3. The planes stack in an  $AB'AB'$  stacking sequence with lines of particles in one plane centered between lines in the plane below. In PUT simulations, the flow deviates dramatically from a Couette form. Large blocks of planes move together and the shear is localized between these blocks. This “blocking” reflects an inherent linear instability when  $d\sigma/dDe < 0$ . Regions which slip more rapidly feel less stress and accelerate. Slower regions are decelerated. This blocking may occur in molecular systems.<sup>2</sup> However, the water surrounding colloidal particles adds a positive contribution to  $d\sigma/dDe$  which stabilizes Couette flow. In any case, all thermostats produce nearly the same phase boundary (within 10%) for  $De > 0.4$ .

Xue and Grest also found a reentrant ordered phase in their Brownian dynamics simulations of colloids.<sup>21</sup> The phase appeared at temperatures above the equilibrium melting transition and at higher  $De$  ( $\geq 2.5$ ) than in Fig. 1. Lines of particles ordered into a close-packed array in the  $\hat{v}$ - $\hat{e}$  plane with no order along the lines. Similar structures have been found in sheared molecular fluids.<sup>22</sup> In contrast, our results show well-defined close-packed order in the  $\hat{v}$ - $\hat{e}$  planes. Also, the  $AB'AB'$  stacking corresponds to a distorted hexagonal lattice of lines in the  $\hat{v}$ - $\hat{e}$  plane. We varied the shape of our simulation cell to check that this distortion is an intrinsic effect. Brown and Clarke may have observed a similar structure in simulations of sheared soft-sphere crystals, although they

refer to it as hexagonal close packed.<sup>23</sup>

Experiments have studied changes in order through scattering measurements of  $S(\mathbf{k})$ . Individual close-packed planes with lattice constant  $a$  produce Bragg peaks on a triangular lattice with spacing  $4\pi/a\sqrt{3}$  in the  $k_{\parallel}=0$  plane. In an fcc crystal, two-thirds of these peaks vanish by symmetry. Experiments show peaks at the suppressed positions which grow relative to the allowed fcc peaks. We find the same trend. Shear changes the interlayer order and breaks the fcc symmetry.

Changes in the order between layers can be seen by examining the line  $\mathbf{k}\mathbf{a}=2\pi(0,2/\sqrt{3},k_{\parallel})$ . The two fcc twins produce peaks at  $k_{\parallel}=1/\sqrt{6}$  and  $(\frac{2}{3})^{1/2}$ . At low shear rates our time-averaged  $S(\mathbf{k})$  has peaks at both positions, indicating substantial  $ABC$  stacking order. By  $De\sim 0.05-0.1$ , the maximum shifts to a central position,  $k_{\parallel}=(\frac{3}{8})^{1/2}$ , indicating a crossover to  $AB'AB'$  stacking.

To date there are no structural measurements in the region of  $\rho_s$  where melting is not observed. Such studies and searches for the reentrant freezing transition will be important tests of our results. Experiments at even higher  $De$  may reveal interesting new behavior due to hydrodynamic forces.

We thank P. M. Chaikin, G. S. Grest, H. M. Lindsay, D. Ou-Yang, and P. A. Thompson for useful conversations. Support from the Exxon Education Foundation, the NSF through Grant No. DMR85-53271, and an allocation at the Pittsburgh Supercomputer Center is gratefully acknowledged. J.F.B. acknowledges support from the U.S. Department of Energy Contract No. W-7405-Eng-48, and M.O.R. acknowledges support from the Sloan Foundation.

<sup>1</sup>J.-P. Poirier, *Creep of Crystals* (Cambridge Univ. Press, Cambridge, 1985).

<sup>2</sup>P. A. Thompson and M. O. Robbins, *Science* **250**, 792 (1990).

<sup>3</sup>B. J. Ackerson and N. A. Clark, *Phys. Rev. Lett.* **46**, 123 (1981); *Physica (Amsterdam)* **118A**, 221 (1983).

<sup>4</sup>P. Pieranski, *Contemp. Phys.* **24**, 25 (1983).

<sup>5</sup>M. O. Robbins, K. Kremer, and G. S. Grest, *J. Chem. Phys.* **88**, 3286 (1988).

<sup>6</sup>B. J. Ackerson, J. B. Hayter, N. A. Clark, and L. Cotter, *J. Chem. Phys.* **84**, 2344 (1986).

<sup>7</sup>H. M. Lindsay and P.M. Chaikin, *J. Phys. (Paris), Colloq.* **46**, C3-269 (1985).

<sup>8</sup>P. M. Chaikin, J. M. di Meglio, W. D. Dozier, H. M. Lindsay, and D. A. Weitz, in *Physics of Complex and Supermolecular Fluids*, edited by S. A. Safran and N. A. Clark (Wiley-Interscience, New York, 1987), p. 65; H. M. Lindsay, Ph.D. thesis, University of California at Los Angeles, 1988 (unpublished).

<sup>9</sup>S. Alexander, P. M. Chaikin, P. Grant, G. J. Morales, P. Pincus, and D. J. Hone, *J. Chem. Phys.* **80**, 5776 (1984).

<sup>10</sup>D. J. Evans, in *Computer Modeling of Fluids, Polymers and Solids*, edited by C. Catlow, S. Parker, and M. Allen (Kluwer Academic, Dordrecht, The Netherlands, 1990), p. 125.

<sup>11</sup>Charles Cleveland, *J. Chem. Phys.* **89**, 4987 (1988).

<sup>12</sup>S. Nosé, *J. Chem. Phys.* **81**, 511 (1984).

<sup>13</sup>H. J. C. Berendsen, J. P. M. Postma, W. F. van Gunsteren, A. DiNola, and J. R. Haak, *J. Chem. Phys.* **81**, 3684 (1984).

<sup>14</sup>D. J. Evans and G. P. Morriss, *Phys. Rev. Lett.* **56**, 2172 (1986).

<sup>15</sup>D. Barber and R. Loudon, *An Introduction to the Properties of Condensed Matter* (Cambridge Univ. Press, Cambridge, 1989).

<sup>16</sup>E. J. Meijer and D. Frenkel, *J. Chem. Phys.* (to be published).

<sup>17</sup>D. Ou-Yang and P. M. Chaikin (private communication).

<sup>18</sup>B. Bagchi and D. Thirumalai, *Phys. Rev. A* **37**, 2530 (1988).

<sup>19</sup>S. Ramaswamy and S. R. Renn, *Phys. Rev. Lett.* **56**, 945 (1986).

<sup>20</sup>At very low  $\dot{\gamma}$ , the measured  $\sigma$  dropped below the apparent  $\sigma_y$ , indicating that there is no true yield stress (Ref. 8).

<sup>21</sup>W. Xue and G. S. Grest, *Phys. Rev. Lett.* **64**, 419 (1990).

<sup>22</sup>W. Loose and S. Hess, *Rheol. Acta* **28**, 91 (1989).

<sup>23</sup>D. Brown and J. Clarke, *Phys. Rev. A* **34**, 2093 (1986).